Elementary excitations in condensed oxygen (α,β,γ, liquid) by high-resolution Raman scattering

Jörg Kreutz[1] and Hans J. Jodl[1,2]

[1]*University of Kaiserslautern, Department of Physics, Erwin-Schrödinger-Str., D-67663 Kaiserslautern, Germany*
[2]*European Laboratory for Non Linear Spectroscopy (LENS), I-50019 Sesto Fiorentino, Firenze, Italy*

Elementary excitations (magnon, libron, vibron, and their combinations) of solid and liquid oxygen samples of high optical quality have been investigated by high resolution Raman spectroscopy in the temperature range 10–90 K. From spectra we deduced band frequency, bandwidth, and band shape of all modes as a function of temperature. In particular we registered in a very narrow temperature range $\Delta T < 0.5$ K at the α-β phase transition libron spectra of the α phase as well as of the β phase; from the coexistence of both phases we can unambiguously follow that this phase transition is of first order. We deduced also from Raman spectra hints about the magnetic interaction, like vibron-magnon mode coupling (unexpected broad vibron band in α-O_2), or two libron excitations. A joint analysis of the vibron frequencies of isotopomers in the $^{16}O_2$ sample allows us to describe the key characteristics of the fundamental energy zone (environmental and resonance frequency shifts) in both low temperature phases. The Raman-active phonon sideband of the internal vibrations in α- and β-O_2 is clearly shifted towards higher frequencies compared to the ir-active one; i.e., both kinds of phonon sidebands therefore possess a different physical origin. We determined the integrated intensity of the magnon Raman band as a function of temperature which is proportional to the magnetic order parameter and which can be modeled by the spin-spin correlation function $\langle S_i S_j \rangle$.

I. INTRODUCTION

Solid oxygen—especially its high pressure phases (<120 GPa)—is a unique material. It combines properties of a cryocrystal and a magnet: it transforms from transparent to colored at increasing pressure, changes from an antiferromagnetic to a diamagnetic structure with pressure, becomes a metallic molecular crystal, and even transforms into a superconducting state at higher pressures (see recent reviews[1]). Although there exists a broad literature about solid oxygen at ambient pressure there are still several important open questions which can be answered by high resolution Raman investigations.

Cahill and Leroi[2] measured Raman spectra of the vibron and librons at some selected temperatures for the first time. Bier and Jodl[3] then performed systematic Raman studies and determined the band frequencies, bandwidths, intensities of elementary librational and vibrational excitations and their temperature dependence. Both groups assigned the peaks in low energetic spectra in the α phase to libron modes B_g and A_g. Van der Avoird *et al.*[4] calculated the magnon and libron frequencies of α oxygen to be in satisfactory agreement with experimental data, including a magnetic coupling to standard lattice dynamics for the first time. Prikhot'ko *et al.*[5] unambiguously confirmed the symmetry of libron modes in α-O_2 (43-cm^{-1} mode with B_g, 79-cm^{-1} mode with A_g) and in β-O_2 (51-cm^{-1} mode with E_g) by polarized Raman scattering on oriented single crystals. Admittedly, the spectra that have been assigned to the nondegenerated A_g libron are not symmetric.[2,3] This discrepancy—up to now not discussed in literature—calls for more accurate Raman measurements.

A continuous transformation in frequency and bandwidth from the E_g libron mode in the β phase to the A_g libron mode in the α phase was measured and explained as a soft mode behavior, and therefore as evidence that the phase transition is of second order.[3] In the meantime the character of the α-β phase transition was unambiguously assigned to be of first order by Fourier transform infra-red (FTIR) spectroscopy[6] and by subsequent x-ray studies,[7] but not by Raman scattering.

The B_g libron relaxation was insufficiently described by only one dominant cubic anharmonic interaction term on the basis of rough bandwidth data.[3] Till now, no more accurate bandwidth data were available to establish a more detailed model for the relaxation of all librons. It is necessary to investigate the relaxation process of vibrational excitations by high resolution bandwidth measurements as a function of temperature. But in orientated oxygen phases these are still missing. Only in liquid O_2 (T$=54-150$ K) and in one temperature point in γ-O_2 (T~53 K) did Kiefte *et al.*[8] perform interferometric measurements of the vibration band in Raman scattering and deduce the bandwidth as a function of temperature.

Several investigations focused on the magnon modes in α oxygen by far ir absorption and Raman scattering. Blocker *et al.*[9] found an absorption line at 27 cm^{-1} in the far ir which they assigned to an antiferromagnetic resonance mode. Mathai and Allin[10] observed a low lying mode at 27 cm^{-1} (at 4 K) by Raman scattering and clearly pointed out an isotopic effect at libron modes and no isotopic effect at the mode at 27 cm^{-1}; consequently they attributed it to a magnon mode. Wachter and Wheeler[11] determined a second magnon at ~6 cm^{-1} by ir absorption. From these spectroscopic data they were able to apply the spin wave theory to α-O_2 (antiferromagnetic) and determined the parameters in the exchange energy (A,B: anisotropic constants; J: exchange parameter) and established a dispersion curve $\omega(\vec{k})$ for magnons. Meier *et al.*[12] performed far ir absorption on both magnons as a function of temperature (T$=5-23$ K) and under the influence of a magnetic field (H<15 T). Finally

Pritula *et al.*[13] confirmed, by doping O_2 with N_2 the magnon at 27 cm^{-1} between 8 and 23 K. But to this day there are no temperature dependent scattering data of the magnon excitation, especially of the temperature dependent intensity behavior.

Löwen *et al.*[14] studied, by Raman scattering and FTIR absorption, the vibron-phonon excitations as a function of temperature (5–40 K), whose nature was analyzed and explained later on by Brodyanski *et al.*[15] In the latter publication a vibration of a ''single'' molecule was assumed to be the origin of the ir-active sideband. To prove this assumption precise frequency Raman measurements of sidebands are necessary for a comparison. In addition the resonance and environmental frequency shift of the O_2 vibron have been determined based on the above assumption and compared to vibron frequencies from Raman spectroscopy.[15] In principle, with accurate Raman frequency data of oxygen isotopes vibration in $^{16}O_2$ or vibrational overtones one can achieve this key characteristic of a fundamental vibron zone based on one set of experimental data only (and thus prove indirectly the correctness of the deconvolution procedure of Ref. 15). But there are no isotopic data available. The vibrational overtone ($2\omega_0 \sim 3100$ cm^{-1}) was investigated by Knippers *et al.*[16] in gaseous oxygen, but up to now not in condensed phases.

The structures of solid oxygen phases at ambient pressure are well documented in the literature:[1] The monoclinic α phase below T$=23.8$ K possesses a crystallographic structure C2/m with one molecule per structural cell and two molecules per magnetic cell with a two sublattice antiferromagnetic order. Only a short-range magnetic order exists in β- and γ-O_2. The rhombohedral β phase between 23.8 and 43.8 K is described by the crystallographic structure R$\bar{3}$m with one molecule per cell; magnetically characterized by a quasi-two-dimensional frustrated 120° triangular lattice antiferromagnet. The cubic γ phase (T$_{\gamma\text{-liquid}}=54.4$ K) has a Pm3n structure with eight molecules per cell on two crystallographic positions: 2a (spherelike molecules) and 6c (disklike molecules). The magnetic structure is described by a quasi-one-dimensional antiferromagnet along the 3 axis occupied by disklike molecules.

Although the structures of the low temperature phases are known in the literature, recent spectroscopic results give one reason to dispute. From ir spectra of vibrational overtone of oxygen we got a hint of a possible doubling of the structural cell of α-O_2.[17] Since the high temperature phase for fluorine and oxygen are similar (Pm3n), due to similar molecular and lattice parameters, one may suspect that the low temperature structures are also similar (C2/c).[18] In this structure the molecular axes are slightly tilted relative to the axis perpendicular to the basal plane and possess a two-layer (herringbone) packing. The slope of the molecular axes in F_2 is 11°; if it would exist in O_2 too it must be less than 5° to be consistent with structural data.[18] But then, in oxygen, one would expect a splitting of the vibron line (from vibrational overtone spectra we estimate ~ 0.2 cm^{-1}) and two additional librons. The fact that the vibron splitting was not observed in fluorine whereas the additional librons have been observed[19] is caused by the resolution (1.5 cm^{-1}) of the named measurement. Therefore high resolution Raman measurements (0.01 cm^{-1}) are necessary to clarify the question if the structure of α-O_2 is C2/m or C2/c.

The general aim of our study is trying to fill the missing information from literature about solid oxygen at ambient pressure. Therefore we have performed systematic, precise (with high resolution <0.1 cm^{-1}, wave number accuracy <0.1 cm^{-1}) investigations of all kinds of low energetic excitations (vibron, libron, magnon and their combinations) in solid and liquid oxygen (from 15 to 90 K) by the high resolution Raman scattering technique. In Sec. II, we will describe our experimental procedure. Experimental results and spectra are presented in Sec. III, and their discussion in Sec. IV. We will analyze first the vibron frequency and estimate the key characteristics of vibron energy zone (environmental and resonance shift) in α and β phases. Second, we will discuss the vibron bandwidth and possible relaxation processes. Third, qualities of libron excitations (intensities, frequencies, bandwidths, mode splitting, two-libron excitations) in both low temperature phases will be analyzed. Fourth, we will discuss Raman-active phonon sidebands to vibron in orientational ordered oxygen phases in comparison with sidebands in nitrogen and ir-active sidebands in both substances.

II. EXPERIMENT

The sample gas (purity 99.998%) was filled into a vessel at 2.3 bar and transferred via a capillary into an optical cell with a sample thickness of 4 mm and a diameter of 10 mm. This cell contained a pointed spike at the bottom made out of copper acting as a condensation point for crystal growth. During cooling the cell by a closed cycle He-cryostat the temperature was controlled by a Si diode at the cooling finger and determined by a second calibrated Si diode attached directly to the optical cell (accuracy $<\pm 0.1$ K, absolute temperature ± 0.5 K); we monitored a small positive temperature gradient vertically in the optical cell. This determination of the actual temperature of the sample was confirmed by several independent measurements of the intensity ratio of Stokes and anti-Stokes libron bands in Raman scattering.

Our technique to grow large polycrystalline samples for optical investigations is described in detail elsewhere.[15] In short, every cooling process from gas to α-phase has been performed extremely slow (0.5–1 K/h), the solid sample was annealed slightly below the crystallization point (ΔT ~ 0.1–0.5 K) for about 10–20 h, and we realized again a substantially slow cooling rate (0.05 K/h) at each phase transition region (liquid$\to\gamma$, $\gamma\to\beta$, $\beta\to\alpha$). The optical quality of monoclinic regions of our O_2-samples was investigated by polarized Raman spectra of vibron and libron modes.

Ordinary Raman spectra were excited by an Ar$^+$ laser with 200–300 mW on the sample and registered by a triple spectrometer in conjunction with a CCD camera (Jobin Yvon T64000). The resolution was 0.2 cm^{-1} in the additive mode, and less than 2 cm^{-1} in the subtractive mode, and the frequency accuracy was better than 0.1 cm^{-1} (respectively 0.5 cm^{-1}) due to the calibration lamps used in each spectral run.
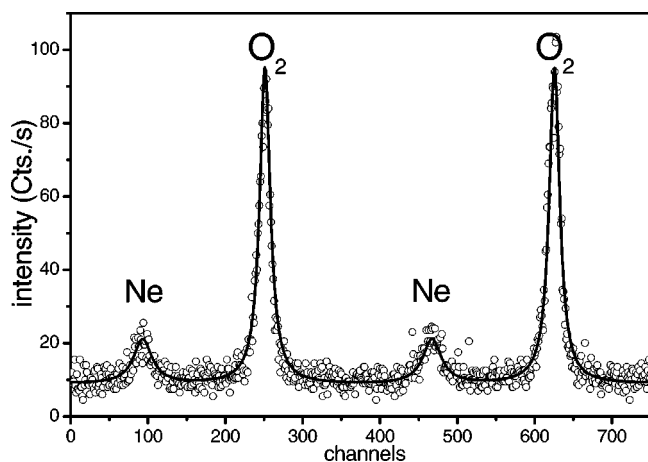
FIG. 1. High resolution Raman spectra of O_2 vibron in the β phase in combination with a Ne atomic line. The free spectral range of the Fabry-Perot-Interferometer is $1.70 \, \text{cm}^{-1}$. The solid line indicates the fit by two Airy functions.

To improve the resolution of a standard Raman system ($\sim 0.5 \, \text{cm}^{-1}$) a single mode laser and a conventional triple monochromator in tandem with a Fabry-Perot interferometer (FPI) and a Peltier cooled photomultiplier for registration were used (achieved resolution $\sim 0.01 \, \text{cm}^{-1}$). This idea goes back to Pine and Tannewald.[20] A specific Raman line (here O_2 vibron at $\sim 1552 \, \text{cm}^{-1}$) was preselected in a conventional manner (slit width $\sim 20 \, \text{cm}^{-1}$) and afterwards the free spectral range (FSR) of the FPI, located in front of the monochromator, was swept mechanically by CO_2 gas pressure. At the position of the intermediate image we used a pinhole of about 100-μm diameter to illuminate the FPI with almost parallel light and to reduce the contribution of stray light. In addition we selected a Ne emission line (528.00853 nm, i.e., $1553.555 \, \text{cm}^{-1}$ relative to the laser line at 487.98 nm) in this free spectral range as an internal standard for determination of absolute Raman frequency values (better than $0.02 \, \text{cm}^{-1}$). Figure 1 shows a typical scan in β oxygen.

The interferogram of the laser line, which we assumed to be infinitely narrow, has been fitted by Airy functions, whose bandwidth we considered to be the apparatus function of the system. The interferogram—containing the oxygen vibron and the Ne calibration line—has also been fitted by two Airy functions. Usually, the difference between the measured bandwidth and the width of the apparatus function delivered the real bandwidth. The error in the bandwidth is of the same order as the spectral resolution, i.e., $0.01 \, \text{cm}^{-1}$.

III. RESULTS AND SPECTRA

A. Region of internal vibrations

The Raman vibron spectrum—presented in a pretty narrow range ($< 2 \, \text{cm}^{-1}$)—is plotted as a function of temperature from 80 to 14 K in Fig. 2. The band frequency decreases in the liquid phase and is quasiconstant in the low temperature regime. In the γ phase, we register the expected splitting into two bands with an intensity ratio 3:1 (six molecules on site c, two molecules on site a). The bandwidth shows a clear temperature dependence; in the liquid and γ phases it is
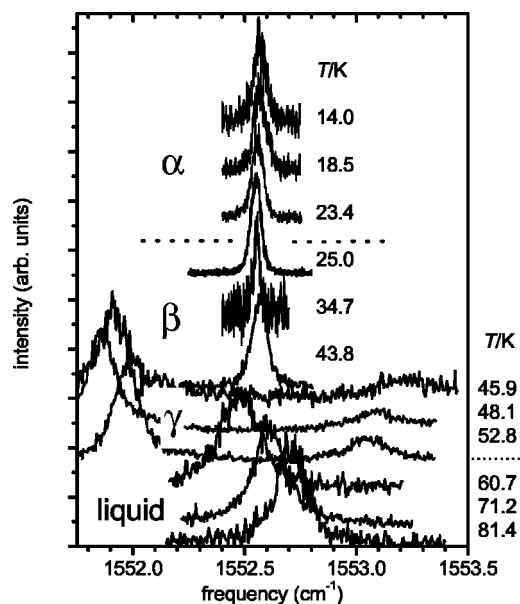

FIG. 2. Qualitative high resolution Raman spectra of oxygen vibron as a function of temperature in liquid, γ, β, and α phases.

much larger than in the α or β phase. Since we performed all these studies over several weeks, we are not able to compare Raman intensities directly.

The vibron in the α phase shows no splitting in high resolution spectra (resolution: $0.01 \, \text{cm}^{-1}$); therefore one can exclude the hypothesis that α-O_2 possesses the same structure as α-F_2 (C2/c; see Sec. I) with the utmost probability. Furthermore, neither additional librons in Raman spectra nor optical phonons in ir spectra have been observed.[21] Therefore we trust in the collinear orientational arrangement of the molecular axes in α-O_2 (namely, C2/m).

Figure 3 shows vibrational Raman spectra of the oxygen isotopes. The position of band frequency of isotopes is needed later (Sec. IV A) to determine environmental and resonance frequency shift. The relative Raman intensities $[I(^{16}O_2):I(^{16}O^{18}O):I(^{16}O^{17}O) \approx 250:1:0.2]$ confirm the natural abundance in O_2 gas we used (99,52:0,41:0,07). We
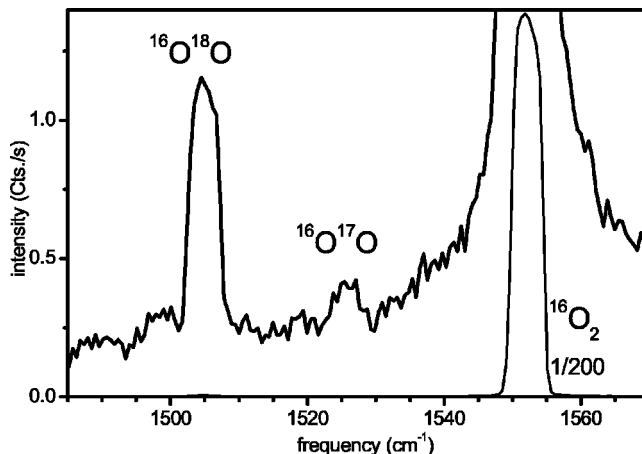

FIG. 3. Vibrational Raman spectra of isotopes in β-O_2 (spectral resolution $\sim 4 \, \text{cm}^{-1}$).
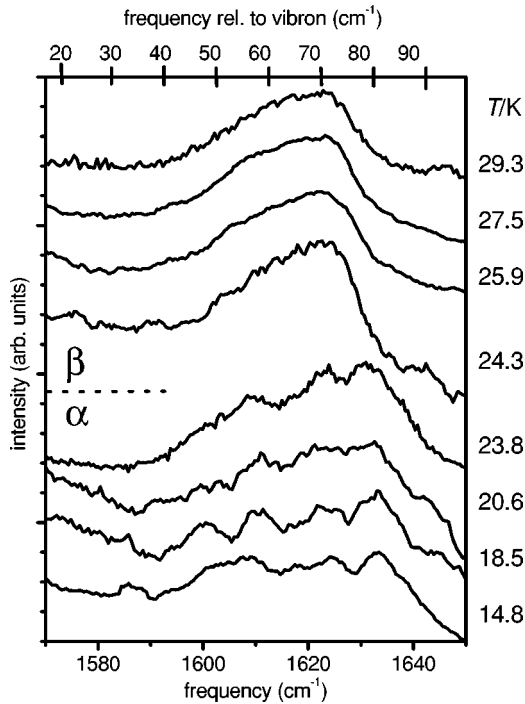
FIG. 4. Temperature dependent Raman spectra of the phonon sideband to the oxygen vibron in β and α phases.
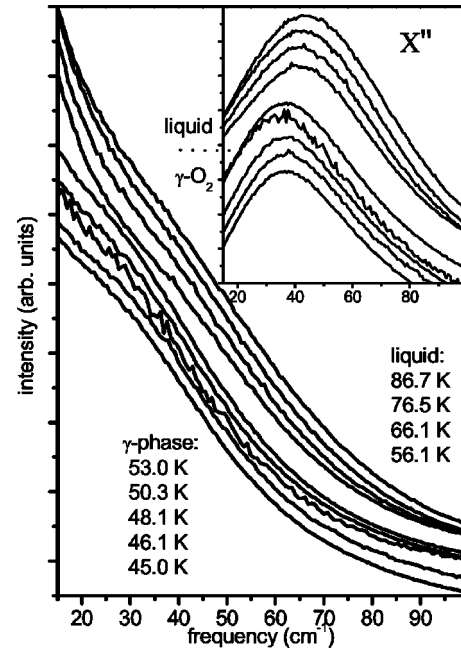

FIG. 5. Close to the Rayleigh line: Raman spectra of γ- and liquid oxygen as a function of temperature. The inset shows the corresponding susceptibility spectra.

determined the $^{16}O_2$ band position to be at 1552.56 cm^{-1}, the position of $^{16}O^{17}O$ at 1525.5 cm^{-1} and the one of $^{16}O^{18}O$ at 1505.0 cm^{-1} with an uncertainty of 0.5 cm^{-1} (literature values in another isotopic mixture for comparison:[22] 1552.7, 1524.6, and 1504.2 cm^{-1}). The band position of the $^{16}O^{18}O$ vibration as a function of temperature shows a pretty constant behavior between 14 and 30 K and no frequency jump at the α-β phase transition ($T_{\alpha\beta}=23.8$ K) which corresponds to structural measurements in which there is no remarkable volume change at $T_{\alpha\beta}$.[18] This fact—that we do not register a frequency jump of the oxygen isotopes at $T_{\alpha\beta}$—is not contradictory to earlier results that a very small CO impurity ($\sim$40 ppb) in solid O_2 clearly shows such a small frequency jump of the CO vibration (0.09 cm^{-1}) at this phase transition.[6(a)] Because the spectral resolution in this ir measurement was higher by a factor of about 50 than in our actual Raman investigations, we can not exclude that there also exists a small jump ($\leqslant$0.1 cm^{-1}) in the vibrational frequency of isotopes.

By different mechanisms (mechanical or electrical anharmonicities), all phonons may couple to a vibron and be detected by optical spectroscopy as sidebands (SBs). Raman spectra of SBs in the α and β phases are plotted as a function of temperature in Fig. 4. This broad feature shows a small temperature shift ($\sim$0.2 cm^{-1}/K) in size and sign like the pure libron modes. The sideband in the α phase is broader and more pronounced than the one in the β phase. The Huang Rhys factor S, which describes the strength of a coupling ($S:=\ln[I_{SB}/(I_{vibron}+I_{SB})]$), is $\sim$0.03 (i.e., weak coupling) and is constant in this temperature range. We could confirm previous data reported by Bier and Jodl.[3] The intensity of the Raman-active phonon sideband spectra in α-nitrogen[23] delivers the same result for coupling in α and β

oxygen: $S(O_2)\sim S(N_2)\sim0.03$. Since we know that the Raman cross sections σ of both substances are almost the same [$\sigma(O_2)_{liquid}=1.05$, $\sigma(N_2)_{liquid}:=1$],[24] we can compare these Raman results directly with results from FTIR absorption. Whereas by Raman scattering sideband intensities of O_2 and N_2 are comparable, the ir spectra show a dramatically different sideband ratio: $I_{SB}(O_2)/I_{SB}(N_2)\approx20$. We will discuss this interesting feature later (see Sec. IV D).

B. Region of external motions

In this low energetic region of Raman spectra we present experimental data of three types of elementary excitations: hindered rotations/torsions in the liquid and γ phases, libron modes in α and β phases, and magnon modes in the α phase, respectively. Figure 5 shows spectra below 100 cm^{-1} at 45–90 K with a typical so called Rayleigh wing of a liquid and/or plastic phase. A qualitative comparison of Raman spectra of the liquid phase to the γ phase shows, first, a much steeper intensity profile I (ω) below 25 cm^{-1} in the liquid phase than in the γ phase, and, second, some sort of a maximum at 45 cm^{-1} in the liquid phase and one at 35 cm^{-1} in the γ phase. Modeling the Stokes/anti-Stokes Raman spectra at 87 K (liquid-O_2) by a free rotor spectrum clearly shows that there must be additional elementary excitations in the liquid besides free rotors. Light scattering spectra for liquid/glass transitions are generally described by susceptibility spectra: i.e., $X''(\omega)=I_{measured}/[n(\omega)+1]\approx\omega\cdot I_{measured}$ for low frequencies; $n(\omega)$ is the Bose factor.[25] This specific representation allows a study of time processes to identify a transition from a liquidlike to a solidlike dynamics on a molecular scale. The inset of Fig. 5 depicts this type of representation of original spectra. Now the difference between
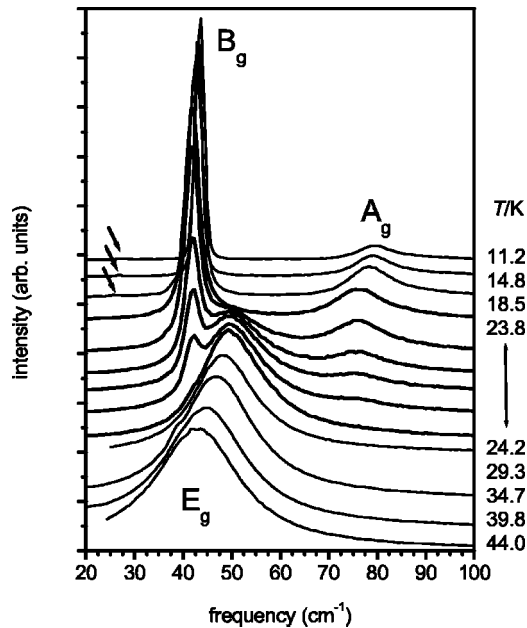
FIG. 6. Libron spectra in the α and β phases as a function of temperature. In a small temperature interval (23.8–24.2 K) both types of libron spectra are clearly seen. (Arrows indicate the magnon position.)

liquid and plastic phases is more pronounced. The band maximum is almost constant in the γ phase, shows a clear jump of frequency (~ 10 cm^{-1}) at the phase transition, and shifts continuously to higher frequencies with increasing temperature in the liquid phase. The bandwidth of susceptibility spectra broadens with increasing temperature, similar in both phases.

Libron spectra (Fig. 6) confirm known data in the literature (see Sec. I). Systematic measurements during cooling/heating cycles show a clear temperature dependence of Raman intensities. Between 24.2 and 23.8 K we observe both libron spectra: one from the α phase and one from the β phase. This result shows the coexistence of both phases or, in other words, the α-β phase transition is of first order. Against this, Bier and Jodl[3] registered a continuous mode transition from E$_g$ (in the β phase) to A$_g$ (in the α phase) and claimed that this spectroscopic result is a hint for a phase transition of second order. Our result agrees with recent FTIR studies[6] and x-ray studies.[7] A more detailed analysis of librons will be discussed later (Sec. IV C).

The magnon spectrum at about 27 cm^{-1} (arrows in Fig. 6) is displayed in Fig. 7(a) in comparison with libron spectra. First temperature dependent Raman studies between 11 and 24 K are presented in Fig. 7(b). We confirmed the only known Raman spectrum by Mathei and Allin[10] taken at 4.6 K. The quality of our spectra is demonstrated by a smaller bandwidth than in comparable ir literature.[9,11–13] When raising temperature the magnon frequency is decreasing and its bandwidth is increasing. Although this magnon mode in Raman spectra is very weak we can clearly prove a decrease of the band amplitude towards the magnetic phase transition. In principle the integrated intensity of a magnon mode is proportional to a magnetic order parameter, which is here the spin-spin correlation function $\langle S_iS_j\rangle$. In Fig. 7(c) the tem-
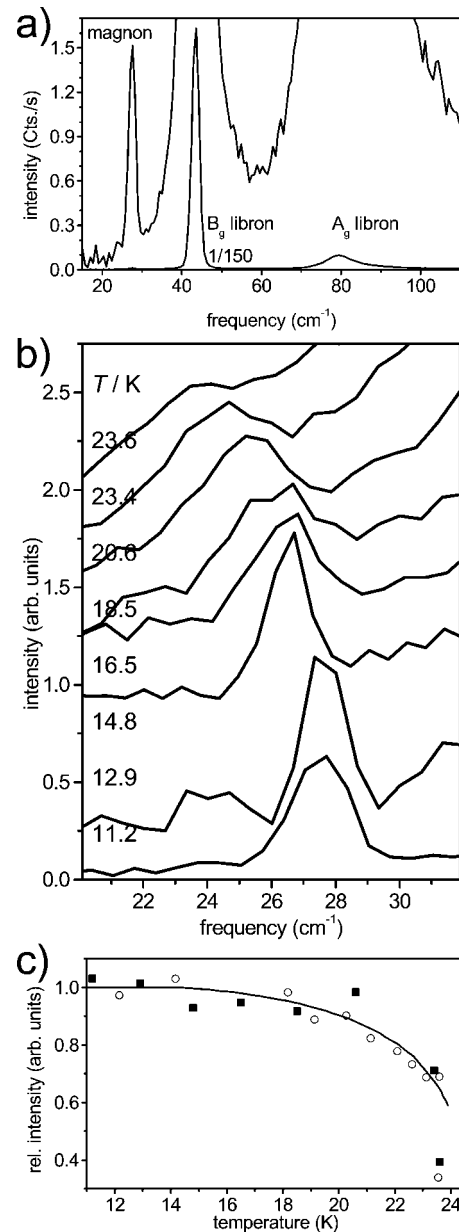

FIG. 7. (a) Raman spectrum of high energetic magnon and librons at T=11.2 K. (b) Temperature dependence of magnon part in whole α phase. (c) Decrease of the normalized magnon band intensity (full squares, uncertainty in Raman intensity is less than 10%) with temperature in comparison to the neutron diffraction peak intensity (open circles, Ref. 26) and the spin-spin correlation function by the Ising model (solid line, Ref. 27).

perature dependence of the magnon Raman intensities is plotted together with magnon peak intensities coming from neutron diffraction studies.[26] The theoretical curve for $\langle S_iS_j\rangle$ [solid line in Fig. 7(c)] following a two-dimensional Ising model on a square lattice,[27] fits all these experimental data quite well in the temperature range T$\leq$23 K. Slightly below the phase transition—between 23 K and 23.8 K—the Ising system is not describing our experimental results properly.

Parallel FTIR studies of the far ir absorption, which provide much better spectra than in Raman scattering, confirm

all the above findings. Therefore we postpone the discussion of our Raman results [Figs. 7(a)–7(c)] including these recent FTIR studies to a forthcoming paper.[21]

IV. DISCUSSION

A. Vibron frequency and vibron zone

Since we were able to measure the vibron frequency with a high accuracy and since it was found to be quasi constant, we are able to plot $\omega(T)$ on a pretty small scale [Fig. 8(a)]. In the liquid, the vibrational frequency $\omega(T)$ shows an S-type behavior, where the frequency at the melting point ($T_m \sim 54$ K) is 0.2 cm^{-1} smaller than at the vapor point ($T_v \sim 90$ K)—a behavior like in nitrogen.[28] In the γ phase the vibron frequencies of both types of molecules (spherelike and disklike molecules) possess a clear temperature dependence, whereas in β and α phases it is more or less constant. The temperature dependence of the vibron splitting $\Delta\omega = \omega_1 - \omega_2$ in the γ phase was determined here in the whole temperature range and follows a mathematical linear fit: $\Delta\omega = 2.53 - 0.03$ T [T in K, $\Delta\omega$ in cm^{-1}; inset in Fig. 8(a)]. We have to consider two different possibilities as an origin of this vibron splitting: First the temperature dependent changes in the interaction between different types of molecules and second the splitting caused by different crystalline fields for molecules on different sites. The latter one is described by the mere volume change with temperature and most important for vibron splitting.[29] The above dependence $\Delta\omega(T)$ delivers, in combination with structural data V(T),[18] a mainly linear dependence of molar volume V:

$$\Delta\omega = 13.71 - 0.55 \cdot V,$$

where $\Delta\omega$ is in cm^{-1} and V in cm^3/mol. Now let us apply this equation for the energy splitting to higher pressures. Since the molar volume was not measured explicitly in the high pressure γ phase we have to estimate it first. The molar volume of β-O$_2$ at 5.5 GPa and room temperature is 14.69 cm^3/mol.[30] With the volume jump of $\sim 5.5\%$ (from zero pressure data) (Ref. 18) at $T_{\beta\gamma}$ one can expect the molar volume in the room temperature γ phase at around 5.5 GPa: $V \approx 15.5$ cm^3/mol. The previous equation $\Delta\omega(V)$ delivers, with this volume, a vibron splitting of 5.2 cm^{-1} at p = 5.5 GPa. This value is in very good agreement with Raman spectroscopic results of Refs. 29 and 31. They reported consistently a splitting of ~ 5 cm^{-1} at 4.8 GPa and 271 K.

If the hypothesis from Brodyanski and Freiman[32] was right—that the local order of the plastic γ phase (spheres and disks) was preserved in the liquid phase—one would expect, in low temperature liquid ($V \approx 24.5$ cm^3/mol given that $\Delta V \sim 4.2\%$ at $T_{\gamma\text{-liquid}}$[34]), a splitting of vibrational lines in the order of 0.25 cm^{-1}. Since the present data were measured with an accuracy of ~ 0.02 cm^{-1} and since these data show no splitting of vibrational line in the liquid (bandwidth ≈ 0.24 cm^{-1}) we can exclude without much doubt that the local order with spherelike and disklike molecules also exists in liquid O$_2$. This inconsistency of theoretical[32] and neutron
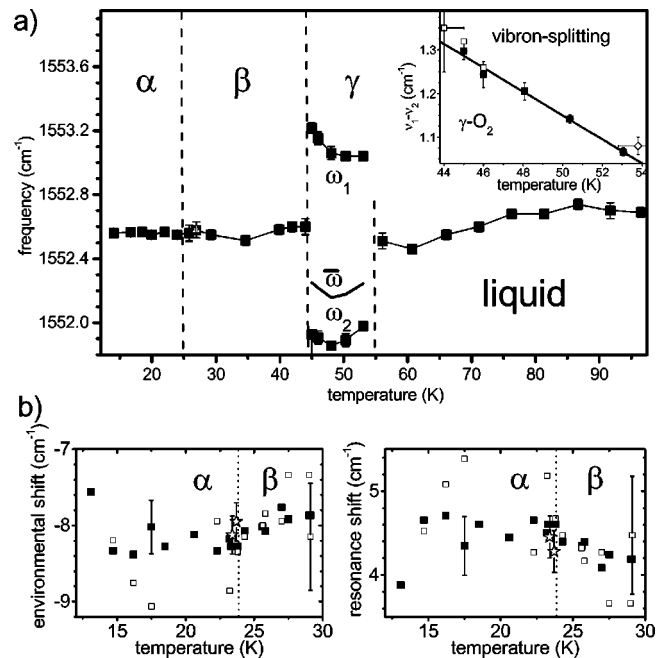

FIG. 8. (a) Temperature dependence of vibron frequency in α, β, γ, and liquid oxygen; insert shows splitting of vibron frequency in γ-O$_2$ as a function of temperature, full squares: our data, open squares from literature: Ref. 3 (≤ 46 K) and Ref. 8(b) (~ 54 K). (b) Resonance shift and environmental shift in α and β phases determined from isotope frequencies: from ^{16}O^{18}O isotope (full squares), from ^{16}O^{17}O (open squares), and from vibrational overtone (stars).

scattering data,[33] on the one hand, and Raman data,[8(a)] on the other hand, was formulated by Dunstetter *et al.*[33] for first time.

Now, if we replace both perturbed frequencies ω_1 and ω_2 by the weighted average $\bar{\omega} = (\omega_1 + 3\omega_2)/4$ [solid line in Fig. 8(a)] then we find a clear frequency minimum in the γ phase at about 48 K and pronounced frequency jumps at both adjacent phase transitions to β and liquid phases. The temperature dependence of the vibron frequency possesses a small but clear local minimum in β and γ phases, measured several times in cooling/heating cycles, which means that one needs at least two different processes which compensate for each other, for explanation. In principle, there are two contributions to the total temperature shift of a mode frequency: first a pure temperature shift at constant volume that originates from temperature dependent potential anharmonicities, and second a shift due to the volume change with temperature. The latter contribution can be derived from temperature dependent data of compressibility and thermal expansion, won from structural investigations,[18] and from the pressure shift of the vibron, won from Raman scattering.[29] The changes of volume dependent frequency shift is relatively small (< 0.04 cm^{-1}) in the whole range of both phases. Therefore, the contribution of phonon-phonon interaction to temperature shift must be very small too.

The vibron frequency shows no significant jump at the α-β phase transition (in which a dramatic spin rearrangement is accompanied by a very small volume change), but a clear jump at $T_{\beta\gamma}$ and $T_{\gamma\text{-liquid}}$. The volume increases $\Delta V \sim 5.5\%$ at $T_{\beta\gamma}$ (Ref. 18) and $\Delta V \sim 4.2\%$ at $T_{\gamma\text{-liquid}}$ (Ref. 34)

are known which alters the distance between neighboring molecules and, therefore, the environmental frequency shift too.

Finally we would like to consider the key characteristics of the fundamental vibron energy zone of oxygen from these Raman data using the isotope frequencies. Due to the literature[35] the solid shift $\Delta\omega$ contains two terms, the environmental and resonance shifts,

$$\Delta\omega := \omega_{solid} - \omega_{gas} = \Delta\omega_{env} + \Delta\omega_{res}.$$

A vibration in an isotope of natural oxygen gas (concentration less than 0.5%) shows all but no resonance shift; therefore, one can determine the environmental shift of the isotope vibration directly. By mass scaling one gets the environmental shift of the $^{16}O_2$-vibron. We determined the environmental shift also from vibrational overtones ($n=2$) because the resonance shift is negligible here [$\Delta\omega_{res}^{(0-n)} = a_n(x_e)^{n-1}\Delta\omega_{res}^{(0-1)}$, with a numerical coefficient a_n of the order of 1 and an anharmonic constant $x_e \approx 0.0076$].[15] With the knowledge of the environmental shift the resonance shift can be obtained from the vibron frequency ($^{16}O_2$). Since we measured the vibron frequency ($^{16}O_2$), the vibrational frequency of both isotopomers ($^{16}O^{18}O$, $^{16}O^{17}O$), and the bivibron of $^{16}O_2$ ($\omega_{0-2} = 3072.25$ cm^{-1}, gas value 3088.5 cm^{-1}) below 30 K, respectively, we were able to determine the environmental shift and the resonance shift by only one spectroscopic method from experimental data [Fig. 8(b)]. The shifts are different in size and sign but temperature independent at the α-β phase transition. The results essentially confirm previous data on frequency shifts of α and β oxygen gained by ir phonon sideband data in comparison with Raman data.[15] This fact indirectly supports the way the band origin frequency was determined in Ref. 15. It also confirms the assumption therein that the zero phonon line corresponds to the frequency of internal vibrations of "single" molecules. Since the error of vibrational frequency shifts is ~ 0.5 cm^{-1} in both cases—isotopomers (Raman, direct) and single molecules (ir, indirect)—we can neither confirm that there is a jump in environmental frequency shift at α-β phase transition as measured in the ir studies of Ref. 15 nor that it is not existing as in our Raman data. Therefore further more exact Raman measurements on the isotopomer are necessary to check if there exists a small jump in Raman data at $T_{\alpha\beta}$. Since these isotope bands are very weak and must be measured with high resolution coherent anti-Stokes Raman scattering (CARS) studies could be suited.

B. Vibron bandwidth and relaxation processes

We measured the Raman Q branch and vibron bandwidth of oxygen at very high resolution below 90 K (Fig. 9). The decrease in bandwidth during warming is typical for a liquid. This behavior was already investigated by Clouter and Kiefte[8(a)] (open circles in Fig. 9) by piezoelectrically scanned Fabry-Perot interferometry. An explanation for the decreasing bandwidth was given in terms of motional narrowing by the authors. With increasing temperature the rotational motion of O_2 molecules is accelerated and, therefore, one molecule "sees" only an average of molecular qualities (like
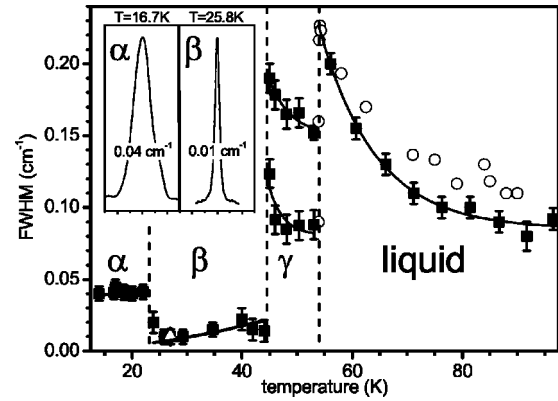
FIG. 9. Vibron bandwidth as a function of temperature in all oxygen phases: full squares, cooling; open triangle, warming; open circles from literature Ref. 8(a); lines in liquid and γ phases are guides to the eye; in β and α phases mathematical fits are due to relaxation processes. The inset shows a direct comparison of the linewidths in these two phases.

electric quadrupole or spin moment) of neighboring molecules. As a result, the found width of the vibration-band decreases with increasing temperature.

The bandwidth of both vibrations in the γ phase are smaller than in the liquid; but they show the same tendency in $\Gamma(T)$ as in the liquid; in addition Γ_{liquid} (at $T_{\gamma\text{-liquid}}$) ~ 0.24 cm^{-1}, Γ_{γ} (of spherelike molecules at $T_{\beta\gamma}$) ~ 0.20 cm^{-1}, Γ_{γ} (of disklike molecules at $T_{\beta\gamma}$) ~ 0.12 cm^{-1}. Our model to describe the decrease in bandwidth is as follows: In a liquid there is no structural order and molecules perform motions of all kinds of freedom (rotations, translations, . . .). Shock freezing of such a liquid would deliver a broad inhomogeneous bandwidth. In the γ phase of oxygen, the molecules possess a structural order (center of mass form a crystal structure), but the molecules are orientationally disordered: spherelike disordered molecules perform rotations in space; disklike disordered molecules rotate only in a plane. Following this line—from liquid to spherelike to disklike molecules—the order is increased, in consequence, the bandwidth is decreased due to lowering entropy.

Since the observed vibron band shape is substantially Lorentzian, we can exclude inhomogeneous broadening, approximately. At the γ-β phase transition we register a clear decrease in the bandwidth ($\Gamma \sim 0.15$ cm^{-1} to ~ 0.01 cm^{-1}), which shows a slight decrease by cooling in the β phase; the extrapolation for $T\to 0$ delivers $\Gamma\to 0$. Therefore, the simplest relaxation channel might be a pure dephasing process: $\Gamma(T) = A \cdot n_p \cdot (n_p + 1)$, with $n_p = n_p(T)$ the occupation number and A the weighted coupling constant.[36] This fit procedure (solid line in Fig. 9) delivers for the coupling constant $A \approx 0.01$ cm^{-1}, whereby the frequency of the mean bath phonon was set to 20 cm^{-1} due to temperature. At the β-α phase transition we observe a clear increase to an almost constant bandwidth in the α phase ($\Gamma \sim 0.04$ cm^{-1})—whereas the vibron frequency shows no discontinuity—while the only effective change in the oxygen crystal is the additional antiferromagnetic spin arrangement. A pure dephasing

process would require a $\Gamma_{homogeneous} \to 0$ for $T \to 0$. So only a depopulation process can explain the finite vibron bandwidth in α phase. The simplest mechanism is a 3-down depopulation process $[\Gamma(T) = B \cdot (n_i + n_j + 1)]$,[36] at which a vibron (1552 cm^{-1}) decays into an $^{16}O^{17}O$ isotopomer vibration (1525 cm^{-1}) and a magnon (~ 27 cm^{-1}). A 3-down depopulation process via phonons is less probable because in the α phase a phonon at 27 cm^{-1} is not populated, and in the β phase dephasing is dominant. The fitting procedure for the relaxation channel vibron→isotopomer+magnon (solid line in Fig. 9) is consistent with measured bandwidth and delivers a coupling constant $B \approx 0.04$ cm^{-1}.

Although the temperature variation of the bandwidth in a limited temperature interval ($\leqslant 20$ K) is very small in both low temperature phases the experimental points $\Gamma(T)$ hardly scatter. Therefore, we are able to establish a model for the relaxation processes of the O_2 vibron. The unexpected wide vibron bandwidth in the α phase is evidence of the direct involvement of a magnetic quasiparticle (a magnon) in the relaxation process of a vibron excitation. To our knowledge, it is the first direct experimental observation of a coupling between vibron and magnon excitations in solid oxygen.

C. Librons in α and β oxygen

1. Libron intensities and two-libron excitations

Looking more carefully at Fig. 6—the spectra of libron modes in α and β phases—we can clearly identify asymmetric band shapes [Figs. 10(a) and 10(b)] and additional very weak broad features [Fig. 10(c)] only at low temperatures. Since there is only one molecule per primitive cell in the β phase, this asymmetry in the E_g mode is due to a lifting of the degeneracy (for a detailed discussion see Sec. IV C 4). The asymmetry in the A_g libron spectrum can be found already in spectra of the literature,[2,3,10] but was not discussed in there. Because this A_g mode is not degenerated there must be another explanation for this asymmetry. Zooming in on spectra of the α phase (Fig. 6) by a factor of 40 we find two broad (>20 cm^{-1}) maxima around 125 and 155 cm^{-1} [see Fig. 10(c)]. It is unreasonable that these bands represents the two-phonon density of states (DOS); looking at the one-phonon DOS (cp. with sideband, Fig. 4) these features here are too small in bandwidth, the bandmaxima deviate and the intensity ratios are different. The observed additional excitations in Raman spectra lie close to those values which are expected for two-libron excitations: $A_g + B_g$ (78 cm^{-1} + 43 cm^{-1} = 121 cm^{-1}) and $A_g + A_g$ (78 cm^{-1} + 78 cm^{-1} = 156 cm^{-1}). Consequently, one would also expect another combination $B_g + B_g$ (43 cm^{-1} + 43 cm^{-1} = 86 cm^{-1}), exactly what we found the asymmetry of the A_g mode at 87 cm^{-1} [see Fig. 10(b)]. The integrated intensity of all above assigned libron features together in the α and β phases is constant during warming/cooling cycles, i.e., spectra are reproducible, which means that our sample is thermodynamically stable. The relative integrated intensities in the α phase are as follows: $I(B_g):I(A_g):I$ (sum of two-libron excitations) $\approx 3:1:1/10$.

To our knowledge, this is for the first time that two-libron excitations are found in α oxygen. In solid nitrogen only the
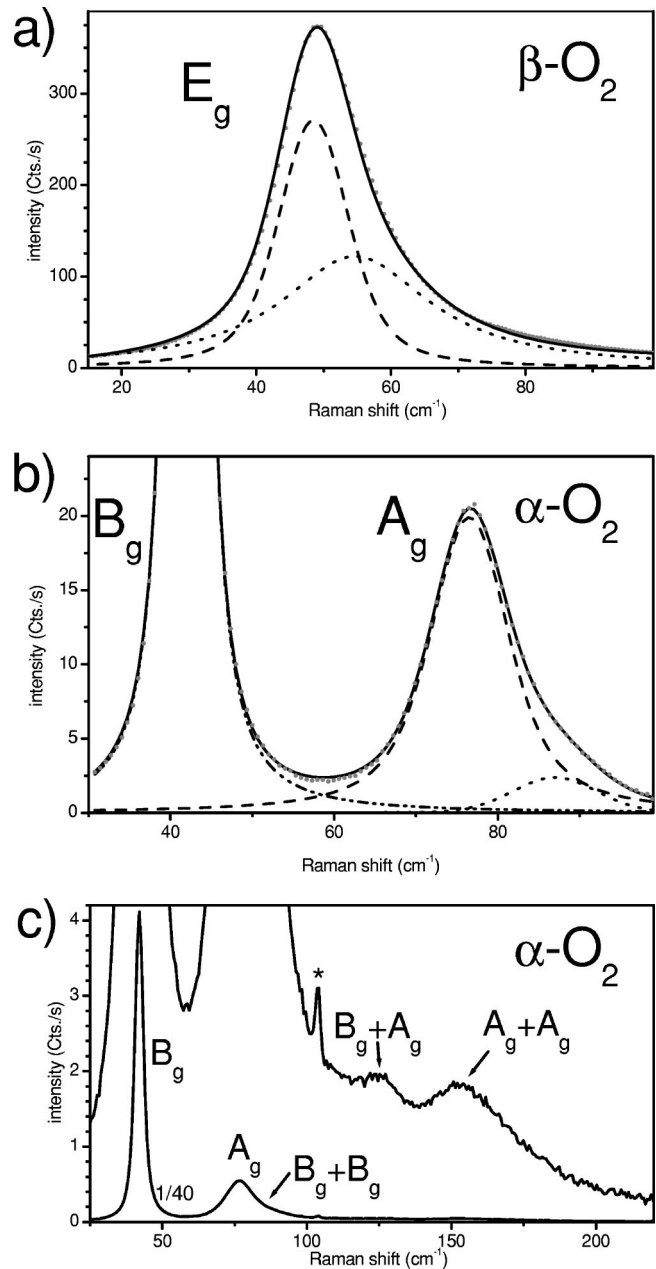

FIG. 10. Raman spectra of libron modes. (a) Asymmetric band shape of E_g libron in low temperature range of the β phase and its deconvolution. (b) The same for the A_g libron. (c) Libron plus libron modes in the α phase (the star marks an Ar-plasma line).

two-phonon DOS was already measured[23,37] and modeled theoretically;[38] but a direct coupling of two quasi-particles has never been observed. Since in β oxygen we were not able to detect similar two-libron bands, these excitations in the α phase are enabled—according to our arguments—only by magnetic coupling of molecules performing librations.

Since an exact deconvolution and separation of these additional very weak Raman librational combination bands is not realizable, we cannot estimate the width of libron energy zone or the libron dispersion. Maybe polarized Raman measurements on oriented single crystals can help to fill this gap.
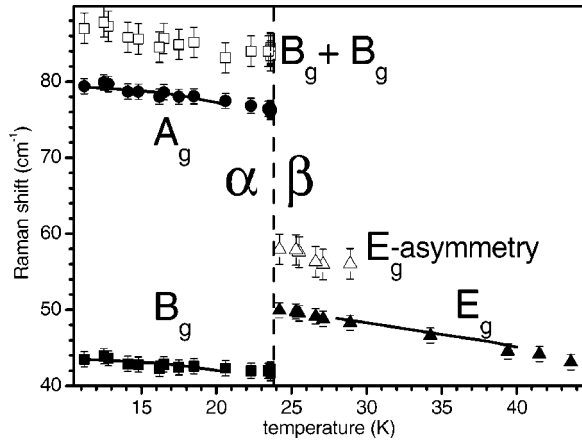
FIG. 11. Raman frequency shift of libron modes as a function of temperature. Solid lines indicate the frequency shift caused by thermal expansion of the lattice in the temperature region of each phase below phase transition.

2. Libron frequencies

The temperature dependence of all modes in the β phase (E_g and E_g asymmetric components) and in the α phase (B_g, A_g, and an unseparated two-libron excitation) are depicted in Fig. 11. Common to all is an almost linear dependence, i.e., a decreasing mode energy with increasing temperature: for E_g: -0.3 cm^{-1}/K, for A_g: -0.3 cm^{-1}/K and for B_g: -0.1 cm^{-1}/K. The two-libron excitation (B_g+B_g) shows the expected temperature shift, which is two times that of the B_g mode. At the phase transition α to β phases we clearly register a pronounced frequency jump within a temperature interval <0.5 K without detectable hysteresis in cooling/heating cycles and not a soft mode behavior as stated before by Bier and Jodl.[3]

As is well known[1(a)] the evolution of libron mode frequencies in oxygen with temperature is determined by three factors. The first factor considers the volume expansion of this phase; the second term is the pure temperature shift, an anharmonic contribution due to phonon-phonon interaction; and the third one is due to the temperature dependent spin-spin correlation function (or magnetic order parameter).

In the case of the β phase the temperature shift of the E_g mode is mostly determined by the thermal expansion of the lattice (solid line in Fig. 11; computation is performed as in the case of vibron frequency: derived from temperature dependent data of the compressibility and thermal expansion, won from structural investigations,[18] and from the pressure shift of the vibron, won from Raman scattering[29]). This result is in agreement with the literature.[18] The pure temperature shift was already calculated numerically in a mean field approximation to be small: $(T \cdot \partial\omega)/(\omega \cdot \partial T) \approx 10^{-3}$.[39]

In the case of the α phase the temperature dependence of the spin correlation function is not negligible any more, in principle. The temperature dependence of frequencies of libron modes A_g and B_g in a range up to 20 K can be explained simply and only by the thermal expansion of the lattice (solid line in Fig. 11, computed as in the case of the E_g mode). The pure (anharmonic) temperature shifts of these frequencies are also negligible in the α phase. It seems that
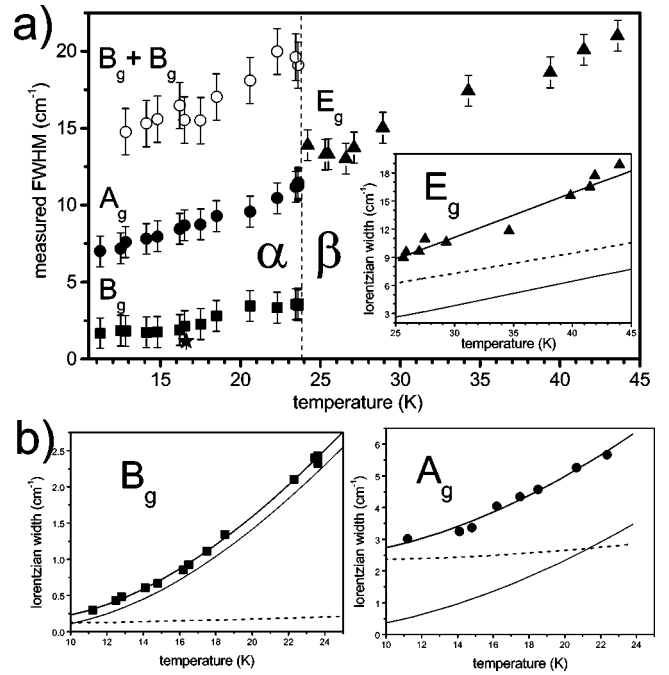

FIG. 12. (a) Measured bandwidth of libron modes as a function of temperature from Raman spectra in α and β phases. (b) [and inset in (a)] Lorentzian part of the corresponding libron bandwidth (full symbols) and its modeling by sum (thick solid lines) of 3-down depopulation (dashed lines) and dephasing (thin solid lines) processes (fit parameters in Table I).

the spin-spin interaction is relevant only in the temperature range near the α-β phase transition (20–24 K).

3. Libron bandwidths

All libron spectra in α and β phases possess a Voigt profile, and we deduced their bandwidth as a function of temperature [Fig. 12(a)]. First we deconvolute this Voigt profile into Lorentzian and Gaussian contributions. The Gaussian part is constant in that temperature region for all modes and originates from the system function (the apparatus function of spectrometer and optics). As we have learned from the vibron bandwidth the quality of our crystal was quite good; therefore we assume a negligible inhomogeneous bandwidth for librons too. The remaining Lorentzian component (Γ_L, of a size equal to the Gaussian one) shows clear temperature dependence [Fig. 12(b)]. The size of $\Gamma_L(B_g)$ (~ 1 cm^{-1} at ~ 17 K) is in accordance with bandwidths particularly determined by HRRS the star in Fig. 12(a) as an example, with an error less than ± 0.1 cm^{-1}—see Sec. II.

Although the measured temperature interval (for the α phase 10–24 K, for the β phase 25–45 K) is small and the change in Lorentzian bandwidth is small but not linear in T for both phases, we are able to draw up possible relaxation mechanisms for libron modes. In both phases (E_g, B_g, and A_g librons) a 3-down depopulation process and a phonon dephasing process are most likely. The inset in Fig. 12(a) and Fig. 12(b) show the fit functions for libron bandwidths in β and α phases [thin solid line: dephasing mechanism $\Gamma(T) = A \cdot n_p \cdot (n_p+1)$ (Ref. 36); dashed line: 3-down depopula-

TABLE I. Raman phonon relaxation process in solid oxygen [due to $\Gamma(T) = A \cdot n_p \cdot (n_p+1) + B \cdot (n_i+n_j+1)$; all values[a] in cm^{-1}].

mode	Dephasing process		Depopulation process	
	ω_p	A	$\omega_i = \omega_j$	B
E_g (~ 50)	30	4.2 ± 0.9	25	3.8 ± 0.6
A_g (~ 78)	20	5.7 ± 0.4	39	2.4 ± 0.1
B_g (~ 42.5)	32.8 ± 2.9	4.4 ± 0.8	21.25	0.11 ± 0.05

[a]Values without errors were chosen as fixed parameters.

tion mechanism $\Gamma(T) = B \cdot (n_i+n_j+1)$ (Ref. 36); thick solid line: sum of both mechanisms; with $n_p(T)$, $n_i(T)$, and $n_j(T)$ phonon occupation numbers and A,B weighted coupling constants; see Table I]. In the β phase both relaxation mechanisms are responsible for modeling the temperature dependence of the bandwidth above 25 K. In the α phase the dephasing process mainly determines the temperature evolution of the bandwidth, whereas the depopulation channel delivers only a more or less constant contribution to the bandwidths [$\Gamma_0(T \to 0)$ is ~ 0.1 cm^{-1} for the B_g libron and ~ 2.4 cm^{-1} for the A_g libron].

4. Libron splitting

To conclude this section about librons, we would like to compare our results to theoretical arguments in literature. According to Raman scattering spectra at the α-β phase transition the twofold degeneracy of the libron spectrum is lifted and the doubly degenerated E_g mode of β-O_2 with frequency 51 cm^{-1} is split into A_g and B_g modes with 79 and 43 cm^{-1}. In the literature[1(a),40] the anisotropic intermolecular potential, which determines the spectrum of librons in the orientationally ordered α and β phases, possess two parts: an exchange part J and a spin independent part of the intermolecular potential U:

$$V_{anis} = U_{anis}(\Omega_1, \Omega_2, R) + J_{anis}(\Omega_1, \Omega_2, R) \cdot \langle S_1 S_2 \rangle,$$

where Ω_1, Ω_2 are unit vectors along molecular axis, R is the vector joining molecular centers and $\langle S_1 S_2 \rangle$ is the spin correlation function.

From an experimental point of view, upon lowering temperature (~ 30 K) in the β phase we observe the asymmetry in the Raman band attributed to the E_g mode. If we deconvolute this asymmetric broad band into two symmetric components we find a component on the high energetic side which is shifted by about $8-10$ cm^{-1} [Fig. 10(a)].

In the literature the influence of the spin dependent anisotropic part was disregarded and the splitting of the E_g mode into A_g and B_g modes in the α phase—due to the anisotropic intermolecular potential U_{anis}—was determined to be ~ 5 cm^{-1} (Refs. 18 and 41) and 11 cm^{-1}.[40] In Fig. 13 the energy level of the libron mode (upper part) is correlated to the intermolecular potential $U(\alpha)$ (α is the angle between perpendicular axis to basal plane and actual molecular axis), which is more complex from left to right (lower part of Fig.
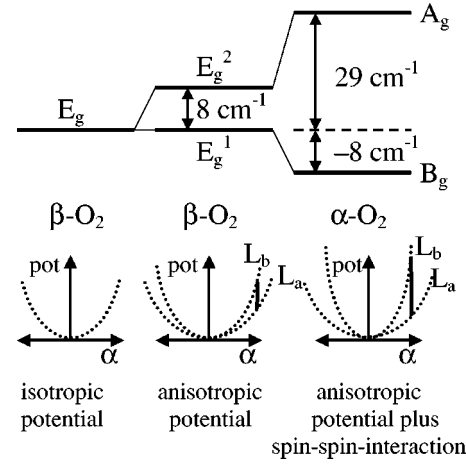

FIG. 13. Scheme to explain the splitting of libron mode in low temperature β and α phases due to different components in anisotropic intermolecular potential $U(\alpha)$; α is the angle between the $c_\perp$ axis and the actual molecular axis.

13). The lowering temperature (around 30 K) kT might be smaller than U_{anis}. At the phase transition $\beta \to \alpha$ both components in the anisotropic potential must be considered, giving rise to the A_g-B_g splitting of the E_g mode due to additional magnetic interaction in the α phase. The strong asymmetric splitting ($\omega_{A_g} - \omega_{E_g} \gg \omega_{E_g} - \omega_{B_g}$; see Fig. 13, top right) is also qualitatively understood following the arguments by Kuchta.[42] If the molecules librate around the b axis (L_b with A_g symmetry) the interaction with four nearest neighbor molecules from the opposite magnetic sublattice is mostly involved, but when they librate around the a axis (L_a with B_g symmetry) the interaction with two next nearest neighbor molecules from the same magnetic sublattice is involved. The latter is much weaker than for the A_g librational mode. As a result, $\omega_{A_g} - \omega_{E_g} \gg \omega_{E_g} - \omega_{B_g}$.

D. Phonon sideband to vibron

As described in Sec. III A the ir-active phonon sideband in oxygen is 20 times more intensive than the one in nitrogen, whereas the intensities of Raman-active sidebands in both substances are comparable. Generally speaking the sideband intensity is proportional to the phonon density of states and a coupling parameter $\chi(\omega)$, i.e., $I_{SB}(\omega) \sim DOS \cdot \chi(\omega)$. This coupling parameter is proportional to the first derivative of a suited intermolecular potential.[35(a)] In case of α-N_2 the intermolecular potential is formed by, e.g., Lennard-Jones and electrostatic quadrupole-quadrupole (EQQ) components. In the case of oxygen, the structure and dynamics are also generated by magnetic interaction. This allows us to explain the differences in ir-active sideband intensities because in oxygen there is an additional contribution to the coupling via magnetic dipole moments. Two further studies report similar results: Gorelli[43] investigated the sideband to a vibron in a high pressure phase (δ, which is similar to the α phase) by FTIR and Medvedev et al.[44] described the sideband to an exciton transition ($\Sigma\Sigma \to \Sigma\Delta$) in α- and δ-O_2 by FTIR. In both cases the authors explained the extremely intensive pho-
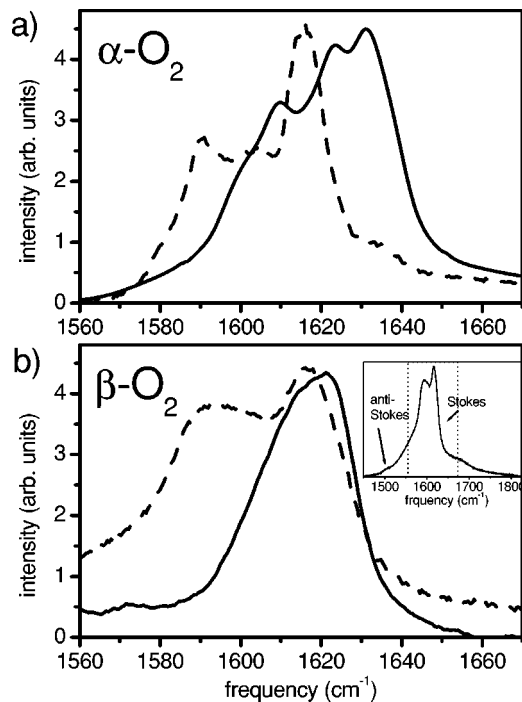
FIG. 14. ir-active phonon sideband (dashed line) to internal vibrations of single O_2 molecules and Raman-active phonon sideband (solid line) to vibron in α and β oxygen. The inset in (b) shows the band overlap of anti-Stokes and Stokes ir-active phonon sidebands in β-O_2.

the case of Raman scattering the phonon sideband is formed by the interaction between two kinds of quasiparticles: vibrons and phonons. Their interaction is not considerably influenced by the spin-spin exchange interaction. In contrast, in the case of light absorption an interaction between internal vibrations of single molecules and lattice excitations was claimed to be responsible for the appearance of an ir-active phonon sideband.[15] Here the spin-spin exchange interaction in solid oxygen mainly contributes to the interaction between intramolecular and lattice excitations.

V. CONCLUSION

We performed extensive, accurate Raman studies with a very high resolution (up to ~ 0.01 cm^{-1}) on all elementary excitations (vibrons, isotopic vibrations, librons, and magnons) and on their combinations (vibron plus phonon, vibron plus vibron, libron plus libron) in the whole temperature range of the α, β, γ, and liquid phases. Due to the excellent crystal quality we were able to determine, from Raman spectra band frequencies, the bandwidth and band shape as functions of temperature for further analysis.

From frequencies of the vibron, isotopic vibrations, and vibrational overtone we estimate the environmental and resonance frequency shift of α- and β-O_2. Our direct results underlay the correctness of the deconvolution procedure of Ref. 15. Therein the zero phonon line was estimated via a deconvolution of Stokes and anti-Stokes components of the ir-active phonon sideband. Also they support the picture that the internal vibrations of single molecules generate the ir-active phonon sideband. A systematic comparison of phonon sideband spectra in the vibron region, measured in Raman scattering or in ir absorption, in O_2 and N_2, proved basic differences in the nature of sidebands detected by both optical spectroscopic methods. The unexpected wide bandwidth of a vibron in the α phase let us clearly deduce the participation of magnon excitation in the vibron decay process, and therefore points up vibron-magnon coupling. Systematic Raman studies of the high energetic magnon (27 cm^{-1}) provide accurate mode frequencies, bandwidths, and band intensities, as functions of temperature (10–25 K). The Raman band intensity as a function of temperature behaves like the temperature dependent spin-spin correlation function. We detected and assigned very weak bands due to two-libron excitations in the α phase and attributed their appearance to the spin-spin exchange interaction part of the intermolecular potential. The asymmetry in the E_g libron of the β phase corresponds to the lifting of this doubly degenerate mode as a consequence of the influence of the anisotropic part of the spin independent intermolecular potential in the low temperature range of this β phase. From the temperature dependence of libron frequencies and bandwidths we describe the libron relaxation qualitatively by 3-down depopulation and dephasing mechanisms. From the coexistence of libron spectra in a very narrow temperature interval at the α-β-phase transition, we were able to characterize this phase transition to be of first order—in contradiction to former Raman studies. Since we detected no splitting of the vibron in the α phase and no additional librons we could exclude a herring-

non sideband coupled to different elementary excitations (vibron or exciton) in compressed oxygen by the additional intermolecular interaction, the exchange interaction. But why are they not different in Raman scattering? Admittedly, this argumentation should work in the traditional picture with both spectroscopic methods. Since the sideband intensities in oxygen by ir and Raman spectroscopy are different we have to renew this picture. Let us therefore describe other features of sideband spectra.

Figure 14(b) shows both types of intensity normalized sidebands in the β phase: with respect to the band origin the ir-active sideband and the Raman-active sideband extend to less than 100 cm^{-1} (in comparison with $\omega_{\text{Debeye}} \sim 80$ cm^{-1}) (Ref. 45); the ir-sideband is twice as broad as the Raman one and possesses a rather substantial anti-Stokes component too (see the inset). Both types of sidebands in the α phase [Raman scattering and ir absorption, Fig. 14(a)] have similar widths (~ 35 cm^{-1}) and four maxima of different height, but the ir sideband is shifted to smaller frequencies (~ 15 cm^{-1}) with respect to the Raman sideband. Differences in both types of sidebands in both phases of α and β oxygen might be due to different direct coupling mechanisms of different phonons from the density of states: in ir absorption more translational modes (lower frequencies) may couple to a vibron, in light scattering more librational ones (higher frequencies). In addition, the band origin (zero phonon line) of the ir sideband is shifted with respect to the one of the Raman sideband.

From intensities and frequencies of ir- and Raman-active phonon sidebands we got the following physical picture. In

bone structure for this α phase as in a similar phase of F_2. From low energetic spectra in high temperature phases we can deduce the large similarity between the liquid and orientational disordered γ phase. Indeed we can negate the continuation of local order from the γ phase to liquid because there is no splitting of the vibrational line in liquid.

[1] (a) Yu. A. Freiman and H. J. Jodl, Fiz. Nizk. Temp. **28**, 691 (2002) [Low Temp. Phys. **28**, 491 (2002)]; (b) Yu. A. Freiman and H. J. Jodl, Phys. Rep. (to be published).

[2] J. E. Cahill and G. E. Leroi, J. Chem. Phys. **51**, 97 (1969).

[3] K. D. Bier and H. J. Jodl, J. Chem. Phys. **81**, 1192 (1984).

[4] A. P. J. Jansen and A. van der Avoird, Phys. Rev. B **31**, 7500 (1985).

[5] A. F. Prikhot'ko, Yu. G. Pikus, L. I. Shanskii, and D. G. Danilov, Pis'ma Zh. Eksp. Teor. Fiz. **42**, 203 (1985) [JETP Lett. **42**, 251 (1985)].

[6] (a) M. Minenko, M. Vetter, A. P. Brodyanski, and H. J. Jodl, Fiz. Nizk. Temp. **26**, 947 (2000) [Low Temp. Phys. **26**, 699 (2000)]; (b) S. A. Medvedev, A. P. Brodyanski, H. J. Jodl, Phys. Rev. B **63**, 184302 (2001).

[7] A. I. Prokhvatilov, N. N. Galtsov, and A. V. Raenko, Fiz. Nizk. Temp. **27**, 532 (2001) [Low Temp. Phys. **27**, 391 (2001)].

[8] (a) M. J. Clouter and H. Kiefte, J. Chem. Phys. **66**, 1736 (1977); (b) H. Kiefte, M. J. Clouter, N. H. Rich, and S. F. Ahmad, Chem. Phys. Lett. **70**, 425 (1980).

[9] T. G. Blocker, M. A. Kinch, and F. G. West, Phys. Rev. Lett. **22**, 853 (1969).

[10] P. M. Mathai and E. J. Allin, Can. J. Phys. **48**, 1518 (1970); **49**, 1973 (1971).

[11] E. J. Wachtel and R. G. Wheeler, Phys. Rev. Lett. **24**, 233 (1970); J. Appl. Phys. **42**, 1581 (1971).

[12] R. J. Meier, J. H. P. Colpa, and H. Sigg, J. Phys. C **17**, 4501 (1984).

[13] I. M. Pritula and L. V. Khashchina, Fiz. Nizk. Temp. **18**, 1035 (1992) [Sov. J. Low Temp. Phys. **18**, 727 (1992)].

[14] H. W. Löwen, K. D. Bier, and H. J. Jodl, J. Chem. Phys. **93**, 8565 (1990).

[15] A. P. Brodyanski, S. A. Medvedev, M. Vetter, J. Kreutz, and H. J. Jodl, Phys. Rev. B **66**, 104301 (2002).

[16] W. Knippers, K. van Helvoort, and S. Stolte, Chem. Phys. Lett. **121**, 279 (1985).

[17] A. Brodyanski, S. Medvedev, M. Minenko, and H. J. Jodl, *Frontiers of High Pressure Research II.*, Proceedings of the NATO Advanced Workshop, Fort Collins (Colorado), USA (Kluwer Academic, Dordrecht, Netherlands, 2001), pp. 217–234.

[18] I. N. Krupskii, A. I. Prokhvatilov, Yu. A. Freiman, and A. I. Erenburg, Fiz. Nizk. Temp. **5**, 271 (1979) [Sov. J. Low Temp. Phys. **5**, 130 (1979)].

[19] T. M. Niemczyk, R. R. Getty, and G. E. Leroi, J. Chem. Phys. **59**, 5600 (1973).

[20] A. S. Pine and P. E. Tannewald, Phys. Rev. **176**, 1424 (1969).

[21] S. A. Medvedev, J. Kreutz, and H. J. Jodl, J. Phys.: Condens. Matter **15**, 7375 (2003).

[22] D. A. Hatzenbuhler and L. Andrews, J. Chem. Phys. **56**, 3398 (1972).

[23] A. Anderson, T. S. Sun, and M. C. A. Donkersloot, Can. J. Phys. **48**, 2265 (1970).

[24] M. Minenko, J. Kreutz, T. Hupprich, and H. J. Jodl (unpublished).

[25] G. Li, W. M. Du, A. Sakai, and H. Z. Cummins, Phys. Rev. A **46**, 3343 (1992).

[26] P. W. Stephens and C. F. Majkrzak, Phys. Rev. B **33**, 1 (1986).

[27] C. N. Yang, Phys. Rev. **85**, 808 (1952).

[28] R. D. Beck, M. F. Hineman, and J. W. Nibler, J. Chem. Phys. **92**, 7068 (1990).

[29] H. J. Jodl, F. Bolduan, and H. D. Hochheimer, Phys. Rev. B **31**, 7376 (1985).

[30] D. Schiferl, D. T. Cromer, and R. L. Mills, Acta Crystallogr., Sect. B: Struct. Crystallogr. Cryst. **B37**, 1329 (1981).

[31] J. Yen and M. Nicol, J. Phys. Chem. **87**, 4616 (1983).

[32] A. P. Brodyanski and Yu. A. Freiman, Fiz. Nizk. Temp. **12**, 1212 (1986) [Sov. J. Low Temp. Phys. **12**, 684 (1986)].

[33] F. Dunstetter, O. Hardouin Duparc, V. P. Plakhty, J. Schweizer, and A. Delapalme, Fiz. Nizk. Temp. **22**, 140 (1996) [Low Temp. Phys. **22**, 101 (1996)].

[34] J. H. C. Lisman and W. H. Keezom, Physica (Amsterdam) **2**, 901 (1935); R. L. Mills and E. R. Grilly, Phys. Rev. **99**, 480 (1955); J. A. Jahnke, J. Chem. Phys. **47**, 336 (1967); L. A. Weber, J. Res. Natl. Bur. Stand. **74A**, 93 (1970).

[35] (a) A. S. Davydov, *Theory of Molecular Excitons* (Plenum, New York, 1971), English translation by B. Dresner; (b) A. D. Buckingham, Proc. R. Soc. London, Ser. A **248**, 169 (1958); Faraday Soc. Trans. **56**, 26 (1960); (c) J. Van Kranendonk, *Solid Hydrogen* (Plenum, New York, 1983).

[36] S. Califano, V. Schettinio, and N. Neto, *Lattice Dynamics of Molecular Crystals* (Springer, Berlin, 1981).

[37] M. M. Thiéry and D. Fabre, Mol. Phys. **32**, 257 (1976).

[38] G. Zumofen and K. Dressler, J. Chem. Phys. **64**, 5198 (1976).

[39] A. P. Brodyanskii, V. A. Slusarev, and Yu. A. Freiman, Fiz. Nizk. Temp. **6**, 533 (1980) [Sov. J. Low Temp. Phys. **6**, 256 (1980)].

[40] A. P. J. Jansen and A. van der Avoird, J. Chem. Phys. **86**, 3583, 3597 (1987); Yu. B. Gaididei, V. M. Loktev, and V. S. Ostrovskii, Fiz. Nizk. Temp. **11**, 740 (1985) [Sov. J. Low Temp. Phys. **11**, 406 (1985)]; Yu. B. Gaididei, V. M. Loktev, V. S. Ostrovskii, and A. P. Prikhot'ko, *ibid.* **12**, 61 (1986) [**12**, 36 (1986)].

[41] I. A. Burakhovich, I. N. Krupskii, A. I. Prokhvatilov, Yu. A. Freiman, and A. I. Erenburg, Pis'ma Zh. Eksp. Teor. Fiz. **25**, 37 (1977) [JETP Lett. **25**, 32 (1977)]; K. Kobashi, M. L. Klein, and V. Chandrasekharan, J. Chem. Phys. **71**, 843 (1979).

[42] B. Kuchta, Chem. Phys. **95**, 391 (1985).

[43] F. A. Gorelli, Ph.D. thesis, Universita degli studi di Firenze, 2000.

[44] S. Medvedev, M. Santoro, F. Gorelli, Yu. Gaididei, V. Loktev, and H. J. Jodl, J. Phys. Chem. B **107**, 4768 (2003).

[45] R. D. Etters, K. Kobashi, and J. Belak, Phys. Rev. B **32**, 4097 (1985).